Bone Reports 24 (2025) 101825

Contents lists available at ScienceDirect

Bone Reports

journal homepage: www.elsevier.com/locate/bonr

Ano5^{Cys360Tyr} mutation leads to bone dysfunction of gnathodiaphyseal dysplasia *via* disturbing Akt signaling

Hongyu Li, Shengnan Wang, Shuai Zhang, Rui Dong, Congcong Miao, Zhenchuan Tian, Ying Hu *

Beijing Institute of Dental Research, Beijing Stomatological Hospital, Capital Medical University, Beijing 100050, China

ARTICLE INFO

Keywords:
Ano5
GDD
Akt
Osteoblast
Osteoclast

ABSTRACT

Background: Gnathodiaphyseal dysplasia (GDD) is a rare autosomal dominant genetic disease characterized by osteosclerosis of the tubular bones and cemento-osseous lesions of the mandibles. *Anoctamin 5* (*ANO5*) is the pathogenic gene, however, the specific molecular mechanism of GDD remains unclear. Herein, a knockin (*Ano5*$^{KI/KI}$) mouse model expressing the human mutation p.Cys360Tyr was used to investigate the role of Akt signaling in enhanced osteogenesis and decreased osteoclastogenesis in GDD.

Methods: Bone marrow-derived macrophages (BMMs) and mouse calvarial osteoblasts (mCOBs) were isolated from homozygous *Ano5*$^{KI/KI}$ mice and treated with SC79, a specific Akt activator. The differentiation and F-actin ring formation of osteoclasts were examined by TRAP and phalloidin staining, respectively. Osteoblast differentiation and mineralization were examined by ALP and alizarin red staining. The expression of bone remodeling-related factors was measured by qRT-PCR.

Results: Akt activation promoted the generation of TRAP-positive multinucleated osteoclasts and the formation of actin rings in *Ano5*$^{KI/KI}$ BMMs cultures, accompanied by increased expression of *Nfatc1*, *Trap*, *Dc-stamp*, *Mmp9*, *Ctsk*, and *Atp6v0d2*. Additionally, *Ano5*^{Cys360Tyr} mutation down-regulated the Akt phosphorylation level in osteoblast. ALP activity and matrix mineralization capacity in *Ano5*$^{KI/KI}$ osteoblast cultures were inhibited after SC79 stimulation, with reduced expression of *Runx2, Opn, Col1a1, and Ocn*.

Conclusion: Akt activation by SC79 stimulation can obviously rescue abnormal increased osteogenesis and decreased osteoclastogenesis in *Ano5*$^{KI/KI}$ mouse model, which demonstrated that disturbed Akt signaling pathway may play a pivotal role in the pathogenesis of GDD, and an Akt activator is probable a therapeutic target for GDD.

1. Introduction

Gnathodiaphyseal dysplasia (GDD; OMIM: 166260) is a rare skeletal syndrome characterized by sclerosis of limb bones and cemento-osseous lesions in mandibles that occurs in an autosomal dominant pattern (Riminucci et al., 2001). *Anoctamin 5* (*ANO5*; *TMEM16E*), encoding a 913 amino-acid protein belonging to the TMEM16 family, was mapped in chromosome 11p14.3–15.1 by linkage analysis and identified to cause GDD (Tsutsumi et al., 2003; Tsutsumi et al., 2005). Recessive mutations in the ANO5 gene cause two types of muscular dystrophies, proximal limb-girdle muscular dystrophy type 2 (LGMD2L) and Miyoshi muscular dystrophy 3 (MMD3) (Penttila et al., 2012). Although ANO5 is involved in various disorders, little is known about the molecular function of the ANO5 protein. Considering that ANO5 is located in the endoplasmic reticulum or cell membrane (Pedemonte and Galietta, 2014; Tran et al., 2014), several lines of evidence have manifested that ANO5 functions as a calcium-activated chloride channels (CaCCs) or phospholipid scrambling protein.

Heretofore, few preliminary studies on the role of ANO5 in bone remodeling have been performed. Research has shown that ANO5 does not affect osteoblast differentiation and mineralization (Kim et al., 2019); on the other hand, XJ Qin demonstrated that *Ano5*-deficient mice exhibited suppressed osteogenesis due to abnormal calcium oscillation, which is divergent from the GDD phenotype (Li et al., 2022a). In fact, most GDD patients are clinically characterized by elevated serum alkaline phosphatase (ALP) levels, a classical measurement of systematic osteogenic activity, and increased bone mineral density (BMD), as determined by radiographic examinations (Sandal et al., 2021; Otaify

* Corresponding author at: Beijing Stomatological Hospital, Capital Medical University, No 4 Tiantan West, Dongcheng District, Beijing 100050, China.
E-mail address: shuaiyu369@163.com (Y. Hu).

https://doi.org/10.1016/j.bonr.2025.101825
Received 18 November 2024; Received in revised form 18 December 2024; Accepted 5 January 2025
Available online 6 January 2025

et al., 2018; Rolvien et al., 2017). However, a consensus is emerging about the association between ANO5 and osteoclastogenesis. *Ano5* knockdown leads to decreased osteoclast differentiation, and its overexpression consistently promotes osteoclast maturation through Akt/nuclear factor of activated T cells 1 (Nfatc1) signaling pathway (Kim et al., 2019; Li et al., 2022a).

The serine/threonine kinase AKT is located downstream of PI3K and undergoes dual activation in the structural domain, which is phosphorylated by phosphoinositide-dependent kinase-1 (PDK1), and the regulatory domain is phosphorylated by mammalian target of rapamycin complex 2 (mTORC2) (Hawkins et al., 1992; Alessi et al., 1996). Subsequently, AKT detaches from the cell membrane to regulate downstream signaling molecules, including GSK3β, Akt1/forkhead box class O (FoxO), and mTORC1, which are generally involved in various biological processes, including cell proliferation, survival, protein synthesis, and metabolism (Manning and Toker, 2017). Notably, the modulatory role of Akt signaling in bone homeostasis has drawn substantial concern. Activation of Akt signaling plays a crucial role in enhancing preosteoblast proliferation, initiating osteogenic differentiation, and promoting the maturation of committed osteoblasts, which is essential for bone morphogenetic protein 2 regulatory function for bone remodeling. (Mukherjee and Rotwein, 2009; Suzuki et al., 2014). As a consequence, Akt1 deficiency in mice leads to osteopenia due to the dysregulation of both osteoblasts and osteoclasts (Kawamura et al., 2007). Furthermore, Akt signaling exerts positive effects on osteoclast differentiation and maturation mediated by increased phosphorylation of GSK3β and nuclear localization of NFATc1 (Moon et al., 2012).

In our previous study, $Ano5^{Cys360Tyr}$ knockin ($Ano5^{KI/KI}$) mice equivalent to the p.Cys360Tyr mutation in a Han GDD family that was firstly reported by our group was successfully generated and partially replicated GDD phenotypes characterized by enhanced osteoblast differentiation and bone formation. Additionally, mice displayed inhibited osteoclastogenesis, which was closely related with early signaling pathways regulated by RANKL-RANK-TNF receptor associated factor 6 (TRAF6) cascades, including Akt, NF-κB, p38, and Erk signaling (Li et al., 2022b). It is worth noting that the phosphorylation of Akt, a classical molecule associated with bone metabolism, was extremely reduced. In the present study, we investigated the effects of the specific Akt activator SC79 on osteoblastogenesis and osteoclastogenesis of mouse calvarial osteoblasts (mCOBs) and bone marrow-derived macrophages (BMMs) from $Ano5^{KI/KI}$ mice and surmised that Akt signaling pathway plays a crucial role in skeletal dysfunction of GDD.

2. Methods

2.1. Generation of $Ano5^{KI/KI}$ mice

The *Ano5* knock-in mouse model (c.1080G > A) was generated by Biocytogen Pharmaceuticals (Beijing) Co., Ltd. A transformation from cysteine into tyrosine at codon 360 of Ano5 was introduced through genomic editing of Clustered Regularly Interspaced Palindromic Repeats (CRISPR)/CRISPR-associated protein 9 (Cas9) technology. Adequate measures were taken to minimize pain and discomfort. All protocols were approved by the Institutional Animal Care and Use Committee of the Beijing Stomatological Hospital (approval number: KQYY-202012-005). $Ano5^{KI/KI}$ mice carrying the p.Cys360Tyr mutation were established through CRISPR Cas9 genomic editing technology. Specifics about the generation and genotype identification of the *Ano5* knock-in mouse model were previously described (Li et al., 2022b). DNA was extracted from mouse tails according to the instructions of a universal genomic DNA kit (CW2298, CWbio, Jiangsu, China), and then genotyping was performed by polymerase chain reaction (PCR). Mice were housed in a pathogen-free environment under a 12-hour light-dark cycle and fed standard food *ad libitum*.

2.2. Isolation and culture of mouse osteoclasts

Wild type and $Ano5^{KI/KI}$ male mice of 6–8 weeks old were sacrificed by cervical dislocation after being deep anesthesia with carbon dioxide narcosis. and their tibias and femurs were collected in PBS. Bone marrow was flushed with alpha-modified minimum essential medium (α-MEM) (12,561,056, Gibco-Invitrogen, New York, USA) containing 10 % fetal bovine serum (10,091,148, FBS; New York, Gibco, USA) and incubated at 37 °C with 5 % CO_2 for 1 day. Nonadherent cells were collected and resuspended in α-MEM supplemented with 30 ng/ml macrophage-colony stimulation factor (31,502, M-CSF; PeproTech, Rocky Hill, USA) to promote BMMs proliferation for 3 days. Subsequently, BMMs differentiated and matured under the stimulation of osteoclast differentiation medium consisting of α-MEM supplemented with 30 ng/ml M-CSF and 100 ng/ml receptor activator of nuclear factor-κβ (RANK) ligand (31511C, RANKL; PeproTech, Rocky Hill, USA). The medium was replaced every other day until the formation of mature multinucleated osteoclasts at day 7. 5 μg/ml AKT activator SC79 (S7863, Selleck, Texas, USA) was treated during the entire differentiation time.

2.3. In vitro osteoclastogenesis assay

To identify mature osteoclasts, BMMs were planked in 96-well plates at a density of 5000 cells/well and cultured with osteoclast differentiation medium for 7 days. Next, the cells were washed with phosphate-buffered saline (PBS) (61,231,114, Gibco, New York, USA) and fixed in 4 % paraformaldehyde (DF0135, Leagene, Beijing, China) for 20 min. TRAP staining was performed according to the manufacturer's instructions (387 A, Sigma Aldrich, New York, USA). Methyl green staining solution is used to stain the nucleus (G1652, Solarbio, Beijing, China). TRAP-positive multinucleated osteoclasts were observed by microcopy (Olympus BX51, Tokyo, Japan). The area featured by multinucleated osteoclasts (≥ 3 nucleus) and TRAP-positive was analyzed by using Image-Pro plus software 6.0. BMMs were also seeded in 24-well plates at a density of 5×10^4 cells/well for phalloidin staining as previously reported. After culture period, the cells were incubated with phalloidin-iFluor 488 (ab176753, Abcam, Cambridge, UK) for 40 min and then with DAPI solution (C0065, Solarbio, Beijing, China) for 5 min to perform nuclear staining. F-actin rings were captured under a fluorescence microscope at Ex/Em = 493/517 nm.

2.4. Preparation of mouse calvarial osteoblasts (mCOBs) culture

mCOBs were isolated from postnatal 1- to 3-day-old female and male littermates after decollation as previously described (Wang et al., 2019). The calvaria were digested in an enzyme mixture containing 2 mg/ml type I collagenase and 0.25 % trypsin for four cycles of 15 min/cycle. Then, the cells were harvested and cultured in α-MEM with 10 % FBS. For osteogenic induction, mCOBs were then cultured in α-MEM supplemented with 10 % FBS, 1 % streptomycin/penicillin (15,140,122, Gibco, New York, USA), 4 μg/ml dexamethasone, 50 mg/ml ascorbic acid and 4 mM β-glycerophosphate (D4902, A5960, and G9422, Sigma-Aldrich, St. Louis, USA). The cultures were changed every two days. 5 μg/ml SC79 was treated during the entire differentiation time. mCOBs were cultured in 6-well plates at a density of 2×10^5 cells/well and used for RNA and protein extraction.

2.5. In vitro osteogenic assay and calcium nodule staining

Osteoblasts were seeded in 6-well plates at a density of 2×10^5 cells per well. After osteogenic induction for 7 days, cells were stained with the ALP staining kit (A59022, Beyotime, Shanghai, China) after fixation with 4 % paraformaldehyde for 30 min, and ALP activity was determined with the OD values at 405 nm on a multifunction microplate scanner. Alizarin red staining was performed for visualization of calcium deposits as previously reported. Briefly, mature osteoblasts with 21-day

osteogenic induction were fixed using 75 % ethanol, and then alizarin red staining solution (1 mg/ml, pH 5.5) (A5533, Sigma-Aldrich, St. Louis, USA) was added. After washing with distilled water, stained cells were photographed. Subsequently, mineralized nodules were incubated with 10 % cetylpyridinium chloride, and absorbance at 562 nm was recorded to examine calcium content.

2.6. Assessment of free calcium in BMMs cytoplasm

For the detection of free calcium in the cytoplasm, BMMs were cultured in 96-well plates at a density of 5×10^3 cells per well. Live cells at different stages of osteoclast differentiation were incubated with CellProbe Fluo-4 AM (S1060, Beyotime, Shanghai, China) for 30 min, and the fluorescence intensity was detected by a microplate reader at an excitation wavelength of 488 nm and an emission wavelength of 516 nm to determine the level of free calcium.

2.7. Quantitative reverse-transcription polymerase chain reaction (qRT-PCR)

Total RNA was isolated using TRIzol reagent (15,596,026, Thermo Fisher Scientific, MA, USA) following the manufacturer's instructions. cDNA synthesis was performed with a SuperRT cDNA Synthesis Kit (CW0471, CWbio, Beijing, China) using one microgram of purified RNA. Synthesized cDNA (1 μl) was used for qRT-PCR analysis with Ultra SYBR Mixture with low ROX (CW3008, CWbio, Beijing, China) on a Bio-Rad thermocycler (Bio-Rad, Hercules, USA) PCR system. The relative expression levels of target genes were calculated using the $2^{-\Delta\Delta Ct}$ method and normalized to the internal control *Actb*. The PCR primer sequences are listed in Supplemental Table S1, Additional File 1.

2.8. Western blot analysis

Cells were harvested and lysed on ice in RIPA Lysis Buffer (Sigma, USA). Coomassie brilliant blue R-250 (Bio-Rad, California, USA) staining solution was employed to measure the protein concentration. Equal amounts (30 μg) of protein from each sample were separated on a 10 % sodium dodecyl sulfate polyacrylamide gel (SDS-PAGE) and transferred onto polyvinylidene difluoride (PVDF) membranes using a Bio-Rad Trans-Blot SD. Membranes were blocked with 5 % nonfat milk and incubated overnight with primary antibodies at 4 °C. Then, horseradish peroxidase (HRP)-conjugated secondary antibody at a dilution of 1:5000 was used for 1 h. The blots were developed with an enhanced chemiluminescent reagent (P10060, NCM Biotech, Suzhou, China) and quantified with a ChemiDoc Touch Imaging System (Bio-Rad, California, USA). Gapdh or Actb was detected as the housekeeping protein. All primary antibodies used are listed in Supplemental Table S2, Additional File 1.

2.9. Statistical analysis

All experiment were performed in triplicate. Statistical analyses were performed using unpaired, two-tailed Student's *t*-test for comparisons between two groups and one-way ANOVA for comparisons of more than two groups using GraphPad Prism 8.0.2 software (GraphPad Software, La Jolla, CA, USA). The results are presented as the mean ± standard deviation (SD). For all experiments, a P value < 0.05 was considered to indicate a statistically significant difference.

3. Results

3.1. Activation of Akt reversed $Ano5^{KI/KI}$ osteoclast differentiation

To further confirm the association of Akt signaling pathway with inhibition of osteoclast differentiation caused by the $Ano5^{Cys360Tyr}$ mutation, the specific Akt activator SC79 was used to treat BMMs from $Ano5^{KI/KI}$ mice. Taken into account the evidence that clinical penetrance between female and male patients with GDD did not show different, wild type and $Ano5^{KI/KI}$ BMMs were cultured from male mice to avoid disturbance of hormone fluctuation. The suppression of Akt phosphorylation was obviously reversed in response to SC79, especially in 15 and 30 min after RANKL induction (Fig. 1a). Importantly, compared with $Ano5^{KI/KI}$ group, the number of TRAP-positive multinucleated osteoclasts with SC79 treatment became more and even up to be comparable with wild-type group, along with sizable enlargement of the spread area in $Ano5^{KI/KI}$ BMMs cultures (Fig. 1b-c). These results indicated that Akt activation could facilitate $Ano5^{Cys360Tyr}$ osteoclast differentiation and maturation.

3.2. Akt activator promoted actin ring formation in $Ano5^{KI/KI}$ osteoclasts

An intact filamentous actin (F-actin) ring structure is a vital process by which differentiated osteoclasts activate bone resorption by attaching to the bone surface and forming a sealing zone (Teitelbaum, 2000). F-actin is composed of a double-helical polymer of monomeric actin (G-actin) in a globular configuration through burning up energy, and phalloidin can specifically bind to F-actin (Akisaka et al., 2001). Phalloidin staining was performed to explore the reverse effect of the Akt activator on osteoclast differentiation and bone resorption. SC79 supplementation into mutant BMMs cultures remarkably rescued actin ring formation and osteoclasts maturation (Fig. 2a-c). Consistently, the Akt activator induced the expression of dendritic cell-specific transmembrane protein (*Dc-stamp*) in $Ano5^{KI/KI}$ BMMs, which is essential for cell-cell fusion and actin ring formation in osteoclasts (Fig. 2d) (Yagi et al., 2005). There is no significant difference at day 3, SC79 stimulation also enhanced the transcription level of the vacuolar (H^+) ATPase (v-ATPase) V0 domain (*Atp6v0d2*) at other stages of osteoclast differentiation (Fig. 2c). Interestingly, it has been reported that Atp6v0d2-deficient mice exhibited representative disruption of osteoclasts fusion similar to *Dc-stamp* knockout mice. In addition, Atp6v0d2 triggers proton transport to the resorptive lacunae and thus preserves the acidic environment needed for bone degradation (Kim et al., 2008; Kim et al., 2009).

3.3. SC79 positively regulated the expression of osteoclastogenesis-related factors in $Ano5^{KI/KI}$ BMMs cultures

Following the formation of an actin ring-rich sealing zone and the presence of a ruffled membrane, bone matrix degradation is induced by osteoclast-specific genes (Boyle et al., 2003). As shown in Fig. 3a, the decreased expression of *Trap*, cathepsin K (*Ctsk*), and matrix metalloproteinase-9 (*Mmp9*) in $Ano5^{KI/KI}$ BMMs cultures was switched back by SC79 at various differential stages. Furthermore, these factors have multiple sites recognized by Nfatc1, which is known as a significant regulator of osteoclastogenesis, and the reduction in Nfatc1 was also reversed by SC79 stimulation (Fig. 3b). Notably, the level of cytosolic calcium taking part in robust Nfatc1 activation was obviously decreased, which was also rescued due to SC79 intervention (Fig. 3c). In brief, these results suggested the negative effects of the p.Cys360Tyr mutation on osteoclast differentiation and function could be rectified by Akt activation.

3.4. SC79 inhibited osteogenic differentiation and mineralization mediated by the p.Cys360Tyr mutation in Ano5

Bone metabolism relies on the delicate balance between bone resorption mediated by osteoclasts and bone formation mediated by osteoblasts. In light of decreased Akt phosphorylation in $Ano5^{KI/KI}$ osteoclasts, we further examined the effects of Akt signaling pathway on the alterations in $Ano5^{KI/KI}$ osteoblast differentiation and mineralization caused by the p.Cys360Tyr mutation. Western blot analysis revealed that the level of Akt phosphorylation was comparable between wild-type

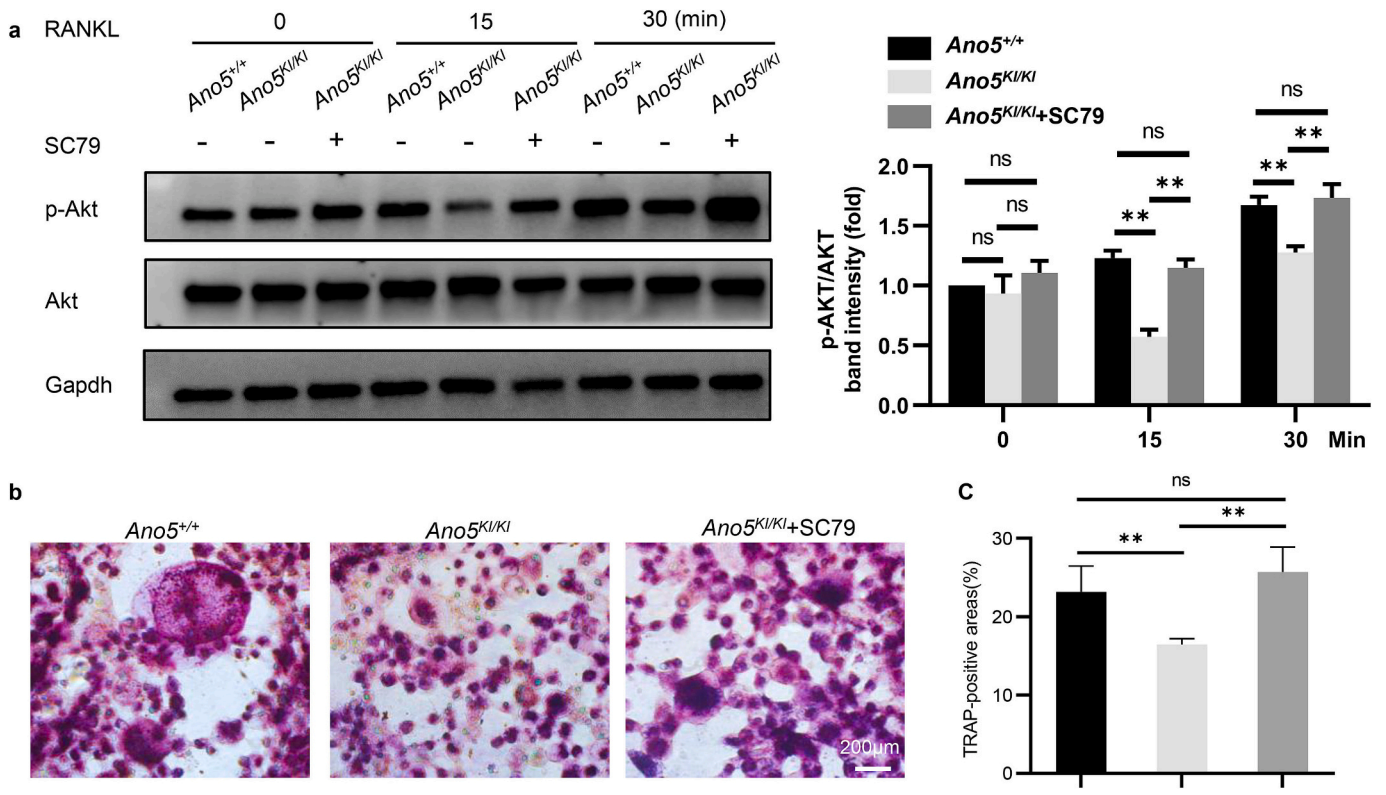

Fig. 1. Akt activation promoted osteoclasts differentiation. (a) Western blot analysis of Akt phosphorylation levels from three groups of $Ano5^{+/+}$, $Ano5^{KI/KI}$, and $Ano5^{KI/KI}$ treated with 5 μg/ml SC79 after 100 ng/ml RANKL stimulation for 0, 15, and 30 min. (b) TRAP and methyl green staining images of mature osteoclasts stimulated with RANKL for 7 days (scale bar = 200 μm). (c) Histogram representing the TRAP-positive area (%) of multinucleated osteoclast (≥3 nuclei). Data are shown as the mean ± standard deviation. $^{*}P < 0.05$, $^{**}P < 0.01$, ns: not significant $P > 0.05$ ($n = 3$).

and $Ano5^{KI/KI}$ osteoblasts at day 0 (Fig. 4a). However, Akt phosphorylation was significantly suppressed in $Ano5^{KI/KI}$ mature osteoblasts after 14 days of osteogenic induction, and this effect was rescued by 5 μg/ml SC79 (Fig. 4b-c). To investigate the intrinsic role of Akt activation on GDD-related enhanced osteogenesis, ALP and alizarin red staining assays were carried out. SC79 stimulation in $Ano5^{KI/KI}$ osteoblasts diminished excessive ALP activity, which is an early marker of osteogenic differentiation (Fig. 4d). Furthermore, extracellular matrix mineralization, the most vital phenomenon in the late stage of bone formation, was detected by alizarin red staining accompanied by the measurement of calcium content, which showed that many fewer mineralized nodules and calcium deposition were formed after $Ano5^{KI/KI}$ cells were cultured with the Akt activator SC79 (Fig. 4e).

3.5. *Akt activation negatively regulated the expression of osteogenic-related factors in $Ano5^{KI/KI}$ mCOBs*

Subsequently, the influences of the Akt activator on transcription levels of bone-forming related factors in different stages of $Ano5^{KI/KI}$ mCOB cultures were explored. We found that up-regulation of *Runx2*, a key regulator of osteoblast differentiation, was reversed almost to the level in $Ano5^{+/+}$ group by SC79 in both undifferentiated and mature $Ano5^{KI/KI}$ mCOB (Fig. 5). Osteopontin (OPN), an important noncollagen protein in bone tissue, is synthesized by osteogenic progenitor cells and bone cells (Si et al., 2020), and the upregulated OPN expression was also inhibited by the Akt activator (Fig. 5). Additionally, osteocalcin (*Ocn*) and collagen type I alpha 1 (*Col1a1*), which are classical markers of late osteogenic factors and matrix maturation, showed similar trends (Fig. 5). Overall, SC79 partially attenuated the enhanced osteogenesis caused by the GDD-related *Ano5* mutation.

Osteoblast could regulate osteoclastogenesis through regulating the expression of RANKL and OPG that is coordinated to regulate bone resorption and density positively and negatively by controlling the activation state of RANK on osteoclasts. Our previous study have found reduced osteoclastogenesis in $Ano5^{KI/KI}$ BMMs partly attributed to elevated Opg/Rankl ratio in osteoblast (Li et al., 2022b). Rankl transcription level with SC79 treatment was equivalent to $Ano5^{KI/KI}$ group (Fig. 5). However, SC79 significantly attenuated Opg expression, which not only promotes bone formation but completes with RANKL to bind with RANK to inhibit osteoclast differentiation and maturation. Consistently, the ratio of Opg to Rankl was obviously declined, implying Akt activation could further rescue osteoclastogenesis in GDD *via* the effect of osteoblast-mediated osteoclastogenesis (Fig. 5).

4. Discussion

In the present study, the Akt activator SC79 promoted the maturation of multinucleated osteoclasts and the formation of intact actin rings in $Ano5^{KI/KI}$ BMMs cultures, suggesting that Akt activation could effectively protect $Ano5^{KI/KI}$ osteoclast function. Furthermore, we observed that abnormally enhanced capacity of osteoblast differentiation and matrix mineralization in $Ano5^{KI/KI}$ mCOB cultures were reversed by an Akt activator, which indicated that Akt signaling is closely associated with aberrant bone remodeling in GDD.

Autosomal dominant mutations in ANO5 are responsible for GDD, which is mainly characterized by enlargement of the mandible, osteomyelitis of the jaws, and cortical thickening of limb bones. In a previous study, we successfully established an $Ano5^{Cys360Tyr}$ knockin mouse model expressing the human mutation p.Cys360Tyr in Ano5, which significantly exhibited typical traits of patients with GDD. Furthermore, $Ano5^{KI/KI}$ mCOB displayed enhanced osteoblastogenesis consistent with our previous study *in vitro* and in another *Ano5* knockout mouse model (Li et al., 2022b; Wang et al., 2019; Jin et al., 2017). The phenotype of impaired osteoclast differentiation and bone resorption in $Ano5^{KI/KI}$

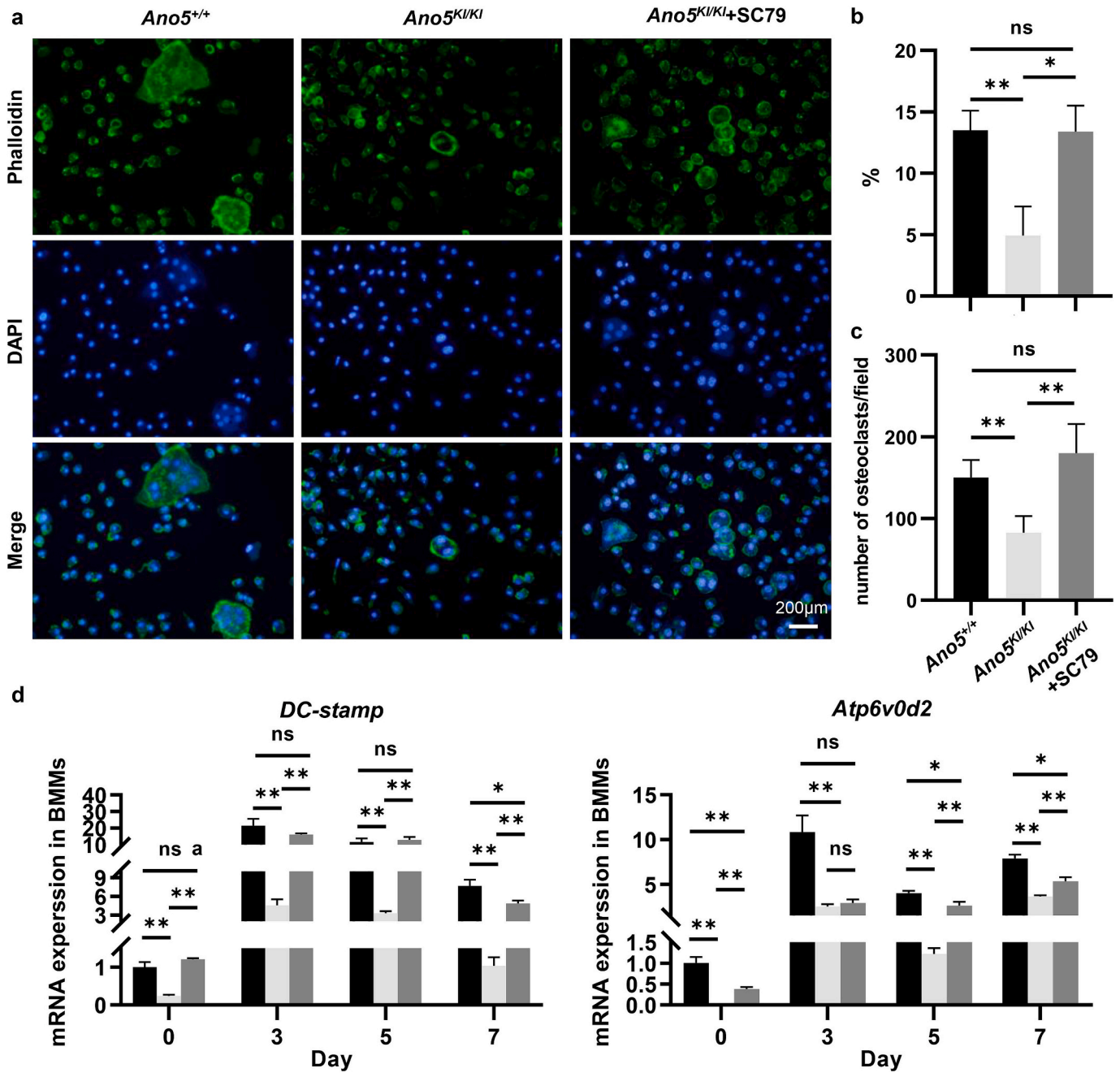

Fig. 2. SC79 motivated *Ano5*^{Cys360Tyr} osteoclasts function *in vitro*. (a) Representative images of actin ring and nuclear staining with phalloidin and DAPI, respectively, in mature osteoclasts cultured with 100 ng/ml RANKL for 7 days (scale bar = 200 μm). (b) The right histogram representing the percentage of nuclei in actin ring-positive osteoclasts *versus* to the total cell numbers. (c) The right histogram representing the number of multinucleated osteoclast (≥ 3 nuclei). (d) qRT-PCR analysis of the cell fusion-related genes *Dc-stamp* and *Atp6v0d2* at days 0, 3, 5, and 7. Data are shown as the mean ± standard deviation. *$P < 0.05$, **$P < 0.01$, ns: not significant $P > 0.05$ ($n = 3$).

mice is highly correlated with the other *Ano5* knockout mice reported by the X, Li group. However, it is currently unclear how *ANO5* dominant mutations lead to the bone disorder of GDD.

Increasing evidence in recent years has indicated that ANO5 is closely associated with osteoclast differentiation and maturation. Consistent with the fact that Ano5 overexpression regulates osteoclast maturation through Akt signaling (Kim et al., 2019), our previous research indicated that the p.Cys360Tyr mutation in *Ano5* significantly inhibited Akt activation. To further determine the association between Akt signaling and abnormal osteoclastogenesis in GDD, SC79 was utilized and rescued the inhibition of TRAP^{-}positive multinucleated osteoclast formation in *Ano5*$^{KI/KI}$ BMMs cultures. The transcription level of *Trap* was also increased with SC79 stimulation. Importantly, enhanced expression of *Nftac1*, a vital transcription factor for osteoclastogenesis, was also observed after Akt activation. The classic NFATc1 activation pathway requires an elevation of the intracellular calcium concentration, which then activates calcium/calmodulin-dependent protein phosphatase calcineurin and in turn leads to robust nuclear translocation of NFATC1 (Kang et al., 2020). Furthermore, a recent study highlighted that *Ano5* deletion in mice significantly diminished calcium oscillations in osteoclasts, which resulted in reduced RANKL-NFATc1 signaling (Li et al., 2022a). Similarly, we found that the free calcium levels in the cytoplasm of *Ano5*$^{KI/KI}$ osteoclasts were lower than those of wild-type osteoclasts and were surprisingly upregulated by SC79

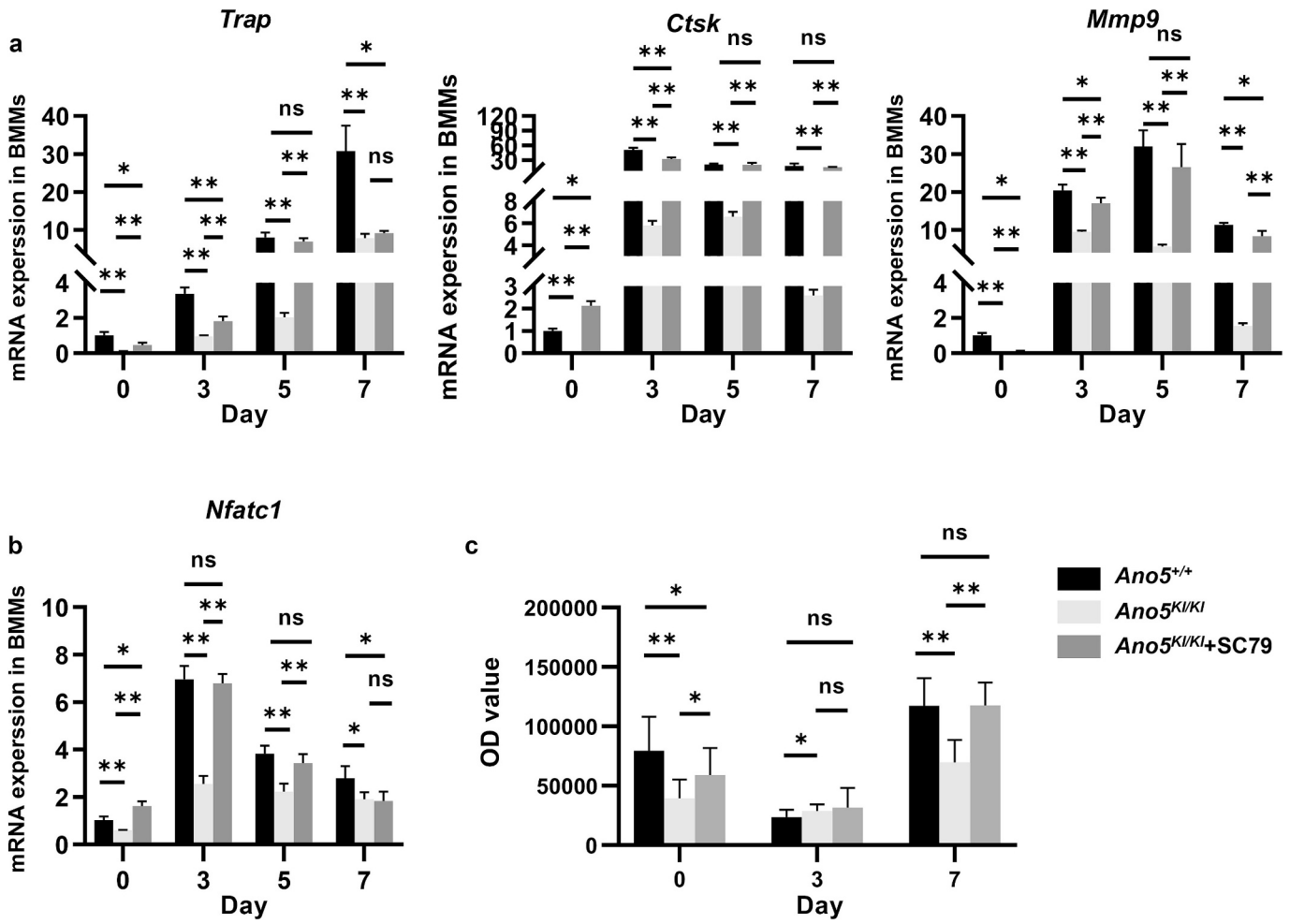

Fig. 3. Akt activation upregulated the expression of osteoclast marker genes in *Ano5*^{Cys360Tyr} BMMs. (a-b) qRT-PCR analysis of *Trap*, *Ctsk*, *Mmp9*, and *Nfatc1* expression in BMMs stimulated with M-CSF (30 ng/ml) and RANKL (100 ng/ml) at days 0, 3, 5, and 7. (c) Statistical analysis of the free calcium content in the cytoplasm at days 0, 3, and 7. Data are shown as the mean ± standard deviation. *$P < 0.05$, **$P < 0.01$, ns: not significant $P > 0.05$ ($n = 3$).

stimulation, which may be attributed to reciprocal feedback between Akt activation and calcium signaling. We found Akt activation also could rescue osteoclastogenesis in GDD *via* declining Opg/Rankl ratio in osteoblast. Our functional evidence further indicated that inhibited osteoclasts differentiation in GDD is closely related with diminished calcium/Nfatc1 cascade pathway that is regulated by inactive Akt signaling.

In the process of osteoclastic bone absorption, multinucleated osteoclasts undergo rearrangements of the actin cytoskeleton to constitute intact actin rings to form a sealed compartment between the bone surface and basal membrane (Boyle et al., 2003). Our *in vitro* data revealed the inhibitory effects of the p.Cys360Tyr mutation on F-actin formation was rescued by Akt activation as well, which was validated by upregulation of *Atp6v0d2* and *Dc-stamp*. Furthermore, the expression of *Mmp9* and *Ctsk*, responsible for the degradation of bone matrix, was enhanced after SC79 stimulation, which further implied that Akt activation could restore the bone resorption ability of *Ano5*$^{KI/KI}$ osteoclasts. These results underscored that inhibition of Akt signaling is a crucial molecule in the abnormal osteoclastogenesis of GDD.

Bone homeostasis also relies on osteoblasts mediating bone formation, and Akt signaling plays a critical role in cell viability, inhibiting apoptosis, and cell differentiation (Mukherjee and Rotwein, 2009). Consistent with the change in osteoclasts, the phosphorylation level of Akt was decreased in mature osteoblasts from *Ano5*$^{KI/KI}$ mice. Meanwhile, our results suggested that SC79 inhibited the ALP activity and mineralized nodules formation of *Ano5*$^{KI/KI}$ osteoblasts, implying that it is crucial for both the early and late stages of osteogenesis. Furthermore, Akt activation obviously suppressed the expression of *Runx2*, a crucial regulator for the proliferation of osteoblast progenitors and their differentiation into osteoblasts and involved in inducing the transcription of *Ocn* and *Col1a1*, which closely take part in the process of bone matrix formation (Komori, 2019).

Canonical AKT signaling is involved in promoting osteoblast proliferation and differentiation through mTOR and Gsk3β/β-catenin cascades (Bai et al., 2021). Nevertheless, the levels of Gsk3β and downstream β-catenin were comparable between *Ano5*$^{KI/KI}$ and *Ano5*$^{+/+}$ mCOBs in our study (Fig. S1, Additional File 1), which indicates that the decrease in Akt phosphorylation regulated osteogenesis by means other than interference of the Gsk3β/β-catenin pathway. Several studies have yielded similar findings to ours and showed that inhibition of Akt phosphorylation with imatinib stimulates osteogenesis in MSCs, but the reason is not well understood (Fitter et al., 2008). Surprisingly, Akt/mTOR signaling could inhibit the autophagy process that is required to maintain osteoblast differentiation and bone matrix secretion. Studies have pointed out that intracellular components of crystal-like structures in the cytoplasm are mainly located in autophagosome-like vesicles, and more convincingly, the apatite crystal components in the vesicles have been identified (Nollet et al., 2014; Guo et al., 2021). We hypothesized that increased osteogenesis caused by the mutation may be due to the reinforcement of autophagic activity. However, our *in vitro* data showed that the p.Cys360Tyr mutation in Ano5 had no relevant effect on the protein level of LC3II, one of the widely used markers for autophagy,

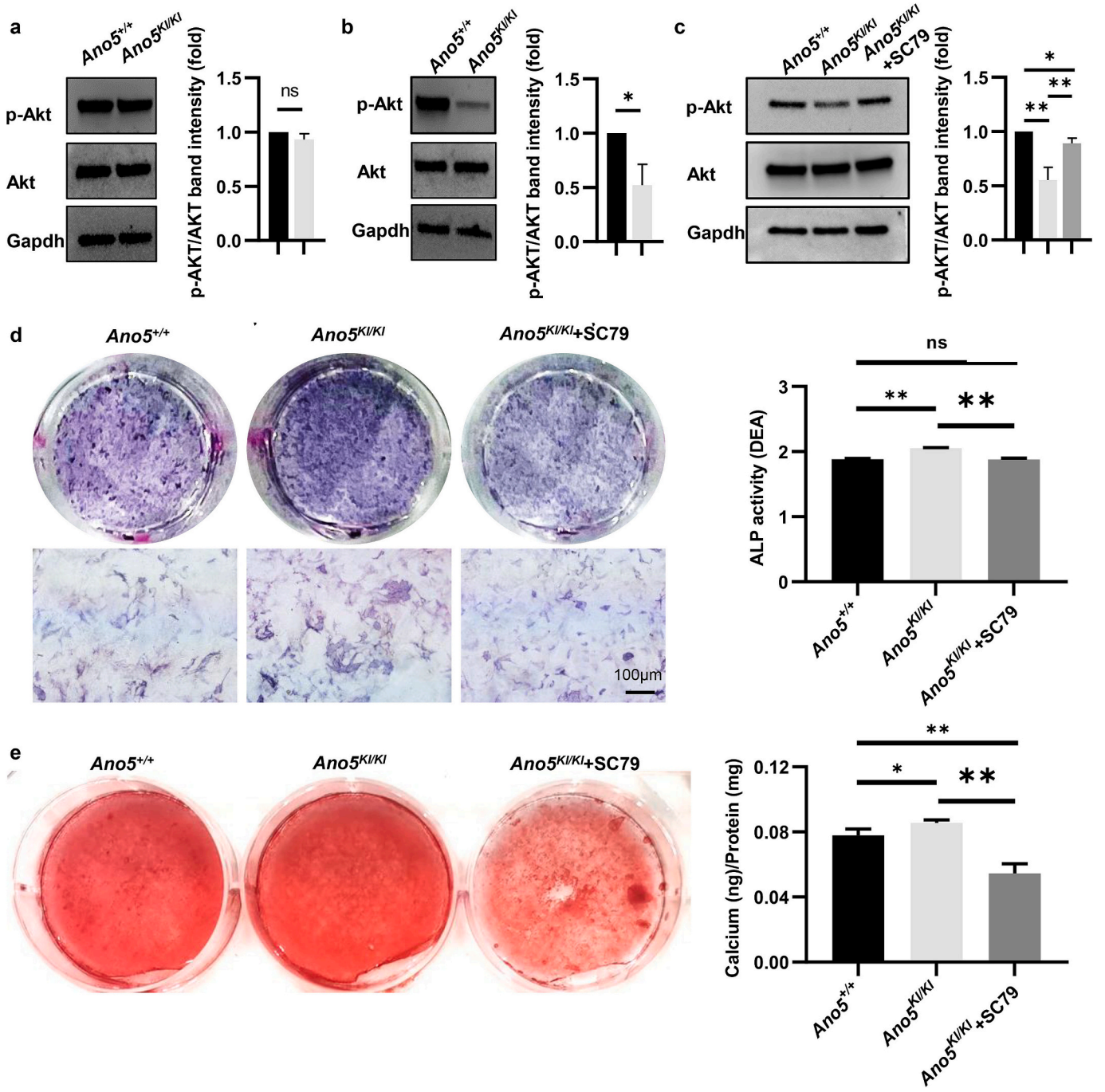

Fig. 4. Akt activation suppressed osteoblasts differentiation and matrix mineralization of *Ano5*^{Cys360Tyr} mCOBs. (a-b) Western blot images of total Akt and phosphorylated Akt levels at day 0 without osteogenic induction (a) and of mature osteoblasts at day 14 (b). (c) Western blot analysis of Akt phosphorylation levels with 5 μg/ml SC79 stimulation in mature osteoblasts. (d) Images of ALP staining from three groups of mCOBs with osteogenic induction for 7 days, and the right histogram representing the quantification of ALP activity (scale bar = 100 μm). (e) Representative images and quantification of AR staining after osteogenic induction for 21 days. Data are shown as the mean ± standard deviation. *$P < 0.05$, **$P < 0.01$, ns: not significant $P > 0.05$ ($n = 3$).

which was further confirmed by comparable levels of *Atg5*, *Atg7*, *Atg12*, and *Beclin-1* (Fig. S2, Additional File 1). The enhanced osteoblastogenesis in *Ano5*$^{KI/KI}$ mCOBs is independent of autophagy and Gsk3β signaling, while specific factors mechanically contributing to excessive osteoblast differentiation and bone matrix secretion mediated by reduced Akt phosphorylation in the GDD disorder model need to be further explored.

5. Conclusion

Our present study reveals that Akt activation modulates abnormal bone remodeling in the GDD model by stimulating osteoclast differentiation and inhibiting osteoblast function. Although the detailed mechanism has not been fully elucidated and further research is needed to verify our findings *in vivo*, this study not only provides a deeper understanding of the pathogenesis of GDD but also lays a new theoretical foundation for targeted molecular therapy.

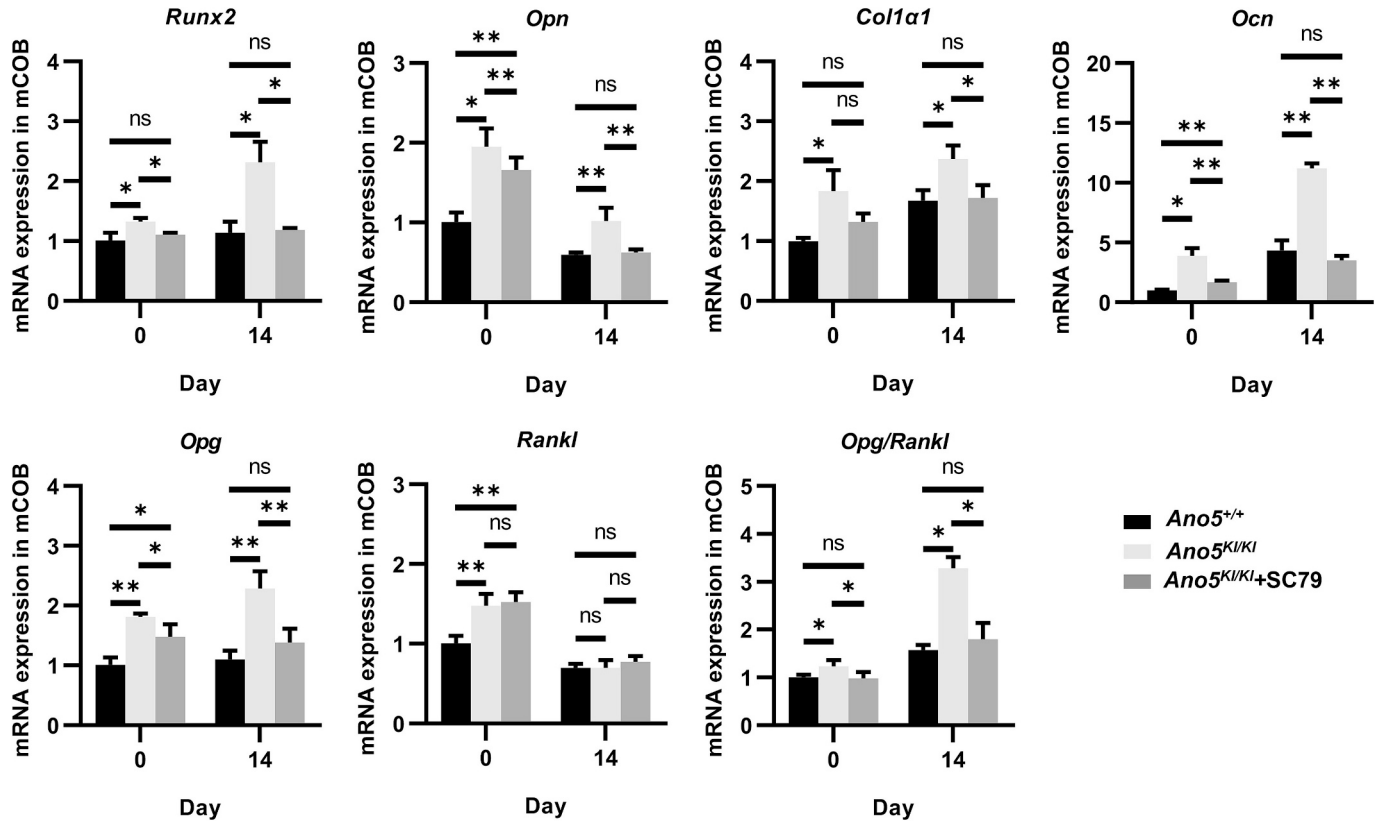

Fig. 5. SC79 rescued the abnormal expression of osteoblast-related genes in $Ano5^{KI/KI}$ mCOBs. Relative mRNA expression of *Runx2*, *Opn*, *Col1a1*, *Ocn*, *Opg*, *Rankl*, and the ratio of *Opg/Rankl* in mCOBs at days 0 and 14 after osteoblast differentiation. *$P < 0.05$, **$P < 0.01$, ns: not significant $P > 0.05$ ($n = 3$).

CRediT authorship contribution statement

Hongyu Li: Writing – review & editing, Writing – original draft, Funding acquisition, Formal analysis, Data curation, Conceptualization. **Shengnan Wang:** Data curation. **Shuai Zhang:** Formal analysis. **Rui Dong:** Formal analysis. **Congcong Miao:** Methodology. **Zhenchuan Tian:** Methodology. **Ying Hu:** Writing – review & editing, Writing – original draft, Funding acquisition, Conceptualization.

Ethics approval and consent to participate

All methods were carried out in accordance with relevant guidelines and regulations. This study is reported in accordance with the ARRIVE guidelines. Overall animal experimental designs and protocals were approved by Institutional Animal Care and Use Committee of the Beijing Stomatological Hospital (approval number: KQYY-202012-005).

Consent for publication

Not applicable.

Funding

This study was funded by the National Natural Science Foundation of China (Grant #82071103, Grant#81570958) and Young Scientist Program of Beijing Stomatological Hospital, Capital Medical University, YSP202317.

Declaration of competing interest

The authors declare that they have no known competing financial interests or personal relationships that could have appeared to influence the work reported in this paper.

Acknowledgments

We gratefully acknowledge all individuals for participating in this study and for institutional support from the Beijing Stomatological Hospital, Capital Medical University.

Appendix A. Supplementary data

Supplementary data to this article can be found online at https://doi.org/10.1016/j.bonr.2025.101825.

Data availability

The dataset supporting the conclusions of this article is available at our institution contacting the corresponding author.

References

Akisaka, T., et al., 2001. Organization of cytoskeletal F-actin, G-actin, and gelsolin in the adhesion structures in cultured osteoclast. J. Bone Miner. Res. 16, 1248–1255.
Alessi, D.R., et al., 1996. Mechanism of activation of protein kinase B by insulin and IGF-1. EMBO J. 15, 6541–6551.
Bai, Y., et al., 2021. Conditional knockout of the PDK-1 gene in osteoblasts affects osteoblast differentiation and bone formation. J. Cell. Physiol. 236, 5432–5445.
Boyle, W.J., et al., 2003. Osteoclast differentiation and activation. Nature 423, 337–342.
Fitter, S., et al., 2008. Long-term imatinib therapy promotes bone formation in CML patients. Blood 111, 2538–2547.
Guo, Y.F., et al., 2021. The role of autophagy in bone homeostasis. J. Cell. Physiol. 236, 4152–4173.
Hawkins, P.T., et al., 1992. Platelet-derived growth factor stimulates synthesis of PtdIns (3,4,5)P3 by activating a PtdIns(4,5)P2 3-OH kinase. Nature 358, 157–159.
Jin, L., et al., 2017. Three novel ANO5 missense mutations in Caucasian and Chinese families and sporadic cases with gnathodiaphyseal dysplasia. Sci. Rep. 7, 40935.

Kang, J.Y., et al., 2020. The role of Ca(2+)-NFATc1 signaling and its modulation on osteoclastogenesis. Int. J. Mol. Sci. 21.
Kawamura, N., et al., 2007. Akt1 in osteoblasts and osteoclasts controls bone remodeling. PLoS One 2, e1058.
Kim, K., et al., 2008. NFATc1 induces osteoclast fusion via up-regulation of Atp6v0d2 and the dendritic cell-specific transmembrane protein (DC-STAMP). Mol. Endocrinol. 22, 176–185.
Kim, T., et al., 2009. Adrm1 interacts with Atp6v0d2 and regulates osteoclast differentiation. Biochem. Biophys. Res. Commun. 390, 585–590.
Kim, J.H., et al., 2019. Role of anoctamin 5, a gene associated with gnathodiaphyseal dysplasia, in osteoblast and osteoclast differentiation. Bone 120, 432–438.
Komori, T., 2019. Regulation of proliferation, differentiation and functions of osteoblasts by Runx2. Int. J. Mol. Sci. 20.
Li, X., et al., 2022a. Ano5 modulates calcium signaling during bone homeostasis in gnathodiaphyseal dysplasia. NPJ Genom. Med. 7, 48.
Li, H., et al., 2022b. Introduction of a Cys360Tyr mutation in ANO5 creates a mouse model for gnathodiaphyseal dysplasia. J. Bone Miner. Res. 37, 515–530.
Manning, B.D., Toker, A., 2017. AKT/PKB signaling: navigating the network. Cell 169, 381–405.
Moon, J.B., et al., 2012. Akt induces osteoclast differentiation through regulating the GSK3beta/NFATc1 signaling cascade. J. Immunol. 188, 163–169.
Mukherjee, A., Rotwein, P., 2009. Akt promotes BMP2-mediated osteoblast differentiation and bone development. J. Cell Sci. 122, 716–726.
Nollet, M., et al., 2014. Autophagy in osteoblasts is involved in mineralization and bone homeostasis. Autophagy 10, 1965–1977.
Otaify, G.A., et al., 2018. Gnathodiaphyseal dysplasia: severe atypical presentation with novel heterozygous mutation of the anoctamin gene (ANO5). Bone 107, 161–171.
Pedemonte, N., Galietta, L.J., 2014. Structure and function of TMEM16 proteins (anoctamins). Physiol. Rev. 94, 419–459.
Penttila, S., et al., 2012. Eight new mutations and the expanding phenotype variability in muscular dystrophy caused by ANO5. Neurology 78, 897–903.
Riminucci, M., et al., 2001. Gnathodiaphyseal dysplasia: a syndrome of fibro-osseous lesions of jawbones, bone fragility, and long bone bowing. J. Bone Miner. Res. 16, 1710–1718.
Rolvien, T., et al., 2017. A novel ANO5 mutation causing gnathodiaphyseal dysplasia with high bone turnover osteosclerosis. J. Bone Miner. Res. 32, 277–284.
Sandal, S., et al., 2021. ANO5-associated Gnathodiaphyseal dysplasia with calvarial doughnut lesions: first report in an Asian Indian with an expanded phenotype. Congenit Anom (Kyoto) 61, 25–26.
Si, J., et al., 2020. Osteopontin in bone metabolism and bone diseases. Med. Sci. Monit. 26, e919159.
Suzuki, E., et al., 2014. Akt activation is required for TGF-beta1-induced osteoblast differentiation of MC3T3-E1 pre-osteoblasts. PLoS One 9, e112566.
Teitelbaum, S.L., 2000. Bone resorption by osteoclasts. Science 289, 1504–1508.
Tran, T.T., et al., 2014. TMEM16E (GDD1) exhibits protein instability and distinct characteristics in chloride channel/pore forming ability. J. Cell. Physiol. 229, 181–190.
Tsutsumi, S., et al., 2003. Autosomal dominant gnathodiaphyseal dysplasia maps to chromosome 11p14.3-15.1. J. Bone Miner. Res. 18, 413–418.
Tsutsumi, S., et al., 2005. Molecular cloning and characterization of the murine gnathodiaphyseal dysplasia gene GDD1. Biochem. Biophys. Res. Commun. 331, 1099–1106.
Wang, X., et al., 2019. Genetic disruption of anoctamin 5 in mice replicates human gnathodiaphyseal dysplasia (GDD). Calcif. Tissue Int. 104, 679–689.
Yagi, M., et al., 2005. DC-STAMP is essential for cell-cell fusion in osteoclasts and foreign body giant cells. J. Exp. Med. 202, 345–351.